Assessment of pistachio shell biochar quality and its potential for adsorption of heavy metals

Kostas Komnitsas[1*], Dimitra Zaharaki[1], Ioannis Pyliotis[1], Despina Vamvuka[1], Georgios Bartzas[2]

[1]School of Mineral Resources Engineering, Technical University Crete, Chania, Crete, 73100, Greece
[2]School of Mining and Metallurgical Engineering, National Technical University of Athens, Zografos Campus, Athens, 15780, Greece
[*]Corresponding author email: komni@mred.tuc.gr, tel: +30 2821037686, fax: +30 2821069554

Abstract

In the present study pistachio shells obtained from Aegina island, Greece, were subjected to pyrolysis for the production of biochar. Pyrolysis was carried out over a temperature range of 250–650 ^{o}C for one hour using a heating rate of 10 ^{o}C·min^{-1} and the quality of the produced biochar was assessed by evaluating its main properties, namely pyrolysis yield, pH, volatile matter, char, fixed carbon, ash and C, H, S, N content. Thermogravimetric analysis (TG), X-ray diffraction (XRD), Fourier Transform Infrared Spectroscopy (FTIR) and Scanning Electron Microscopy (SEM) were used for the identification of the morphology and structure of the produced biochar. Finally, the potential of biochar to remove heavy metals, namely Pb and Cu, from solutions was investigated.

Keywords

Biochar, pistachio, pyrolysis, adsorption, heavy metals

Introduction

Biochar is a carbon rich, fine-grained and porous material which is produced by heating organic matter at temperatures not exceeding 700 ^{o}C. Biochar differs from charcoal regarding its final use as a soil amendment to improve soil quality and sequester carbon, whereas charcoal is generally combusted for heating or cooking [1, 2]. Several thermochemical processes, namely conventional or flash carbonization, slow or fast pyrolysis and gasification can be used for the production of biochar from agricultural wastes. Slow pyrolysis has the advantage of retaining almost half of the feedstock carbon in stable biochar [3].

Pyrolysis involves thermal treatment of biomass at temperatures >400 ^{o}C in a low oxygen atmosphere to yield syngas (mainly hydrogen, methane and carbon monoxide), bio-oil (alcohols, oils, tars and acids) and biochar (that contains mainly C and also O, H, N and ash). Syngas or pyrolysis gas can be used as a fuel source to heat the pyrolysis unit. Bio-oil is a carbon-rich liquid fuel which can be used as a substitute for fossil fuels for providing heat, electricity and/or chemicals [4, 5].

Due to its chemical and biological stability, when biochar is applied to agricultural land may improve soil fertility, maintain sustainable production and reduce contamination of streams and groundwater since in several cases has a strong tendency to adsorb contaminants present in soils and thus reduce their leachability. Furthermore, it has the potential to reduce levels of atmospheric carbon dioxide and help countries to meet greenhouse gas emission reduction targets. Biochar is recalcitrant against decomposition and remains in the soil for centuries or millennia, since almost half of its dry biomass weight is pure carbon. It is known that if biomass is left to decompose in air, almost all carbon is lost into the atmosphere within a few years. On the other hand, during pyrolysis, almost 50% of biomass carbon is converted into biochar, while of the other 50% around two thirds are released as useful energy [6, 7].

Biochar can be produced in every country using biomass from biowaste (which includes biodegradable municipal and agricultural waste) or purpose-grown re-growing biomass plantations. In recent years, several studies have been carried out to assess the benefits of using biochar in terms of carbon sequestration and mitigation of global warming as well as to explore its potential as soil amendment to improve soil health and productivity [8-11]. Other recent studies underline the potential of using biochar as adsorbent for the removal of contaminants, mainly organic, from solutions, soils and hazardous wastes [12-14]. Most studies available in literature and dealing with the removal of inorganic contaminants from solutions as well as the use of biochar in hazardous waste management are also recent [15-17].

In the Mediterranean region the life cycle of pistachio, which is produced in orchards of *Pistacia vera L.*, results in the production of considerable amounts of by-products. Only in Greece, the primary processing of these nuts results in over 7000 tons of by-product streams (hulls and shells) which are more than 75% of the harvested crop. Traditionally, these by-products are used either as animal feed, fuel for energy generation (mainly in the US), soil amendment or are discarded as waste.

The present paper aims to assess the quality of biochar produced from pyrolysis of pistachio shells. These and similar types of agricultural by-products/wastes are produced in huge quantities in several countries and regions (US, Mediterranean, Middle East) and may become a noticeable source of biochar that can be used as a) soil amendment in order to improve soil quality and mitigate soil erosion in areas suffering from desertification and b) alternative adsorbent for the clean-up of wastewaters and management of industrial waste. So far, very few studies have been traced in literature regarding the application of pistachio biomass or biochar in environmental applications [18, 19]. Studies on the production and use of biochar derived from other types of nuts are also very rare.

Methodology

Roasted and light salted pistachio shells (PI) were obtained from Aegina island, which is the main pistachio producing area in the country and is situated in the Saronic Gulf, 18 miles off the south coast of Athens, Greece. The raw material was soaked for 6 hours in warm water (60 ^{o}C) to remove most salt and then dried for 24 hours in an oven (ON-O2, MEDLINE) to remove moisture. Then, pyrolysis of small quantities, e.g 50 g, of shells was carried out in a modified laboratory furnace, N-8L SELECTA, at temperatures varying between 250-650 ^{o}C, using porcelain capsules. Nitrogen was fed in the oven at a rate 100 mL·min^{-1} for 60 min to remove air. The heating rate was maintained at 10 ^{o}C·min^{-1} and the retention time of the feedstock in each temperature was 60 min.

Pyrolysis yield (y_P) was determined for all biochars produced at temperatures of 250, 300, 350, 450, 550 and 650 °C (PI250, PI300, PI350, PI450, PI550 and PI650, respectively) from the % weight loss of the mass after pyrolysis. pH and oxidation–reduction potential of PI and biochars were measured using a solid:liquid ratio of 0.25 with a Hanna 211 pH/Eh meter while electrical conductivity (EC) with a Hanna EC215 conductivity meter.

The elemental C, H, S and N analysis was carried out in a Flash 2000 Elemental Analyzer Thermo Scientific calibrated using BBOT standards (2,5-Bis(5-tert-butyl-2-benzo-oxazol-2-yl)thiophene) containing carbon. The oxygen content was subsequently calculated as the difference. Porosity (%) was measured by mercury intrusion porosimetry using a Micromeritics AutoPore 9400 porosimeter.

Pistachio shells (PI) and all biochars were subjected to thermogravimetric analysis using a differential thermogravimetric analyzer TGA-6/DTG of Perkin Elmer (temperature measurement precision of ±2 ºC, microbalance sensitivity <5 μg). The rate and % weight loss for each sample were determined continuously as a function of time or temperature, under dynamic conditions, in the range of 25-850 ºC. The experiments were carried out at atmospheric pressure, under nitrogen/air atmosphere, with a flow rate of 45 mL·min^{-1} and a linear heating rate of 10 ^{o}C·min^{-1}. Volatile matter (VM), char and fixed carbon (FC) content were also determined. All experiments were carried out in duplicate.

X-ray diffraction (XRD) analysis of biochars was performed using a Bruker D8 Advance diffractometer with a Cu tube and a scanning range from 3° to 70° 2θ with a step 0.03° and 4 sec/step measuring time. Qualitative analysis was carried out using the Diffrac$_{plus}$ software (Bruker AXS) and the PDF database. Fourier Transform Infrared Spectroscopy (FTIR) analysis was carried out using a Perkin-Elmer Spectrum 1000 (USA); for the production of the pellets each sample was mixed with KBr at a ratio 1:100 w/w. Scanning Electron Microscopy (SEM) analysis was carried out with a JEOL 6380LV scanning electron microscope equipped with an EDS INCA microanalysis system with low vacuum, pressure 30 Pa, voltage 20 kV and 10 to 12 mm sample distance (working distance) from the detector.

Toxicity Characteristics Leaching Procedure (TCLP) tests were performed for selected biochars (PI300 and PI550) to determine the concentration of heavy metals in the extract and subsequently assess their potential toxicity [20]. Metal concentration was determined through inductively coupled plasma mass spectrometry (ICP-MS), analyzer Agilent Technologies 7500cx.

Adsorption experiments were carried out in 200 mL beakers using pistachio shells (PI) and selected biochars (PI300 and PI550). Four solutions with various concentrations, namely 15, 45, 70 and 150 mg·L^{-1} Pb and Cu were prepared by dissolving the required quantities of $Pb(NO_3)_2$ and $Cu(NO_3)_2 \cdot 3H_2O$, respectively, in distilled water. Four concentrations of the adsorbent PI, PI300, PI550, namely 1, 2, 5 and 10 g·L^{-1}, were used. Tests were also carried out using 1 g·L^{-1} of activated carbon (Donau Chemie, Austria) as control. Agitation took place on a Vibromatic rocking mixer at 350 rpm, at room temperature, until equilibrium was reached (24 h). At various time intervals (0.5, 1, 6, 12 and 24 h) 10 mL of liquid samples were withdrawn and filtered through Whatman filters (0.45 μm) for the determination of Pb and Cu concentrations using a Perkin Elmer Analyst 100 flame atomic absorption spectrophotometer. All tests were carried out in triplicate.

Results and discussion

Characterization of pistachio shells and biochars

Pistachio shell (PI) and biochars PI250, PI300, PI350, PI450, PI550 and PI650 are characterized in Table 1. As seen from these data, pyrolysis yield decreases from 72.9 to 26% as temperature increases from 250 to 650 ^{o}C, respectively.

When temperature is higher than 350 ºC the low pyrolysis yield obtained is due to condensation of aliphatic compounds and loss of CH_4, H_2 and CO. Dehydration of hydroxyl groups and thermal degradation of ligno-cellulose structures also takes place between 550 and 650 ºC. Similar results have been reported regarding the pyrolysis yield of biochars produced from several other agricultural wastes, namely peanut hulls, pecan shells, corncob poultry litter and switchgrass in this temperature range [21, 22].

Table 1. Characterization of pistachio shell (PI) and biochars PI250, PI300, PI350, PI450, PI550 and PI650

	PI	*PI250*	*PI300*	*PI350*	*PI450*	*PI550*	*PI650*
y_P, *%*	-	72.9	49.9	31.6	31.4	28.4	26.0
pH	4.25	4.68	4.96	5.11	6.71	7.15	8.81
EC, mS/cm	7.7	13.1	13.7	21.5	25.9	29.7	33.9
VM, %	86	70.9	49.2	48.1	44.1	28.3	13.9
Char, %	14	29.1	50.8	51.9	55.9	71.7	86.1
FC, %	12.4	27.1	49.0	50.2	54.2	69.9	84.4
Ash, %	1.6	2	1.8	1.7	1.7	1.8	1.7
Porosity, %	15.2	22.3	26.0	27.9	29.6	32.5	34.1
% C	45.93	54.20	66.67	69.98	75	77.25	79.34
% H	6.04	5.34	4.16	3.31	2.84	2.14	1.32
% N	0.42	0.37	0.34	0.23	0.21	0.18	0.05
% O	48	40	29	26	22	20	19

Increased pyrolysis temperature results in increased pH (from 4.68 to 8.81) and EC (from 13.1 to 33.9 mS/cm) for the biochars. Based on the pH values shown in Table 1, it is deduced that biochars produced from pyrolysis at temperatures lower than 350 ºC may be used as soil amendments in alkaline soils, while biochars produced at 650 ºC may be applied in acidic soils. In other studies, pH values up to 8.6 are reported for biochars produced from peanut hulls, pecan shells, reed and switchgrass after pyrolysis at 500 ºC, while if biochars produced from water canna, palm leaf, pineapple peel and weaner manure, pH values can be as high as 11 [23].

The volatile matter content is also negatively correlated with pyrolysis temperature as shown in Table 1, where a gradual decrease from 70.9 to 13.9% is noticed when temperature increases from 250 to 650 ºC. It is mentioned that the high volatile matter content present in biochars produced at low temperatures, where aliphatic-C structures are not affected, usually indicates a low potential of the biochar as soil amendment [3, 24]. The volatile matter content of biochar produced at 700 ºC from pecan shells and poultry litter was reported to be in the range of 10-15%, as reported by Novak et al. [5].

Increase of pyrolysis temperature results also in increased char and FC content, especially for temperatures higher than 300 °C, reaching 86.1% and 84.4% respectively. The ash content, being the difference between char and FC content and denoting the inorganic matter content, varies in all samples between 1.6-2%.

Increased porosity of biochars was shown with increased pyrolysis temperature, reaching at 34.1% at 650 ºC. At higher temperatures porosity increases due to the transformation of aliphatic C structures to aromatic C structures [25, 26].

Increasing pyrolysis temperature, from 250 to 650 ºC, results in increased total carbon content from 54.2 to 79.3%, decreased hydrogen and oxygen content from 5.34 to 1.32% and 40 to 19%, respectively. Nitrogen content decreased from 0.42 to 0.05% due to volatilization. In agreement with the present study, the carbon content of biochars produced from pine chips, peanut hulls and switchgrass at 400-500 ºC was determined at around 80%, whereas when poultry litter was used as raw material the carbon content of the produced biochar was only 40% [27].

According to Laird et al. [4] biochar produced at lower temperatures may have a higher content of bioavailable carbon and available nutrients, which will enhance microbial activity and thus plant growth. However, higher content of bioavailable carbon could result in quick degradation and less sequestered carbon from soils [28].

According to the TCLP test carried out for biochars PI300 and PI550, the concentration of Cr, Pb, Mn, Cu, Cd, Ni and Zn in the solution are very low (<0.06 $mg \cdot L^{-1}$) and do not exceed the thresholds for Cr (5 $mg \cdot L^{-1}$), Pb (5 $mg \cdot L^{-1}$) and Cd (1 $mg \cdot L^{-1}$); no TCLP thresholds have been defined for the other heavy metals. Thus, the toxicity risk from potential biochar application in soil, in terms of heavy metal solubilisation is considered as negligible.

TG and DTG analysis

Figure 1 shows the TG curves for pistachio shell (PI) and biochars PI250, PI300, PI350, PI450, PI550 and PI650. The total calculated weight loss decreases accordingly for biochars produced at higher temperature (86.3, 67.5, 50.7, 41.7, 40.2, 31.7 and 20.5 %, respectively). For all samples, the weight loss during heating up to 250 °C does not exceed 8%. A sharp weight loss is shown for PI and biochar PI250 between 300 and 400 °C, while for biochars PI300-PI650 the weight loss is linear and smooth at temperatures higher than 300 °C.

DTG curves for PI and biochars PI250 and PI300 are presented in Figure 2. DTG curves of the other biochars are not shown due to their similarity with the curve of PI300. The noise shown in some parts of the curves is due to instrumental difficulties.

Two distinct peaks are clearly shown in the DTG curve of PI, which are typical for pyrolysis of lignocellulose materials. The first peak at around 300 °C represents the decomposition of hemicellulose which decomposes at 150–350 °C. The second peak at around 350 °C corresponds to the decomposition of cellulose which usually takes place in a relatively narrow temperature range of 275-350 °C. The presence of cellulose in PI is also confirmed by the XRD analysis, as discussed below. The gradual decomposition of lignin over a wider temperature range (usually at 275-500 °C) is represented by the flat section [29-31].

The thermal decomposition of biochars PI250 and PI300 was initiated at around 300 °C. For biochar PI250, a major loss of weight is shown at the temperature range of 300-400 °C. This observation confirms also the weight loss shown in Figure 1.

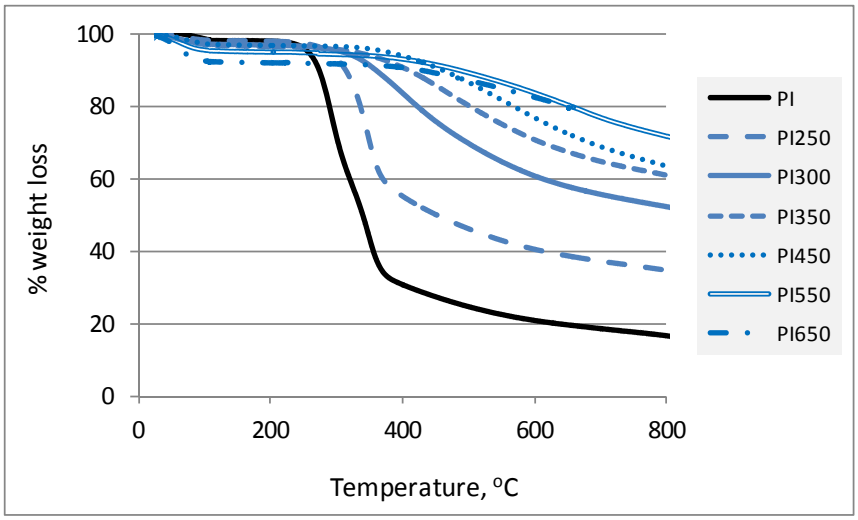

Figure 1. TG curves of weight loss versus temperature for pistachio shells PI and biochars PI250, PI300, PI350, PI450, PI550 and PI650

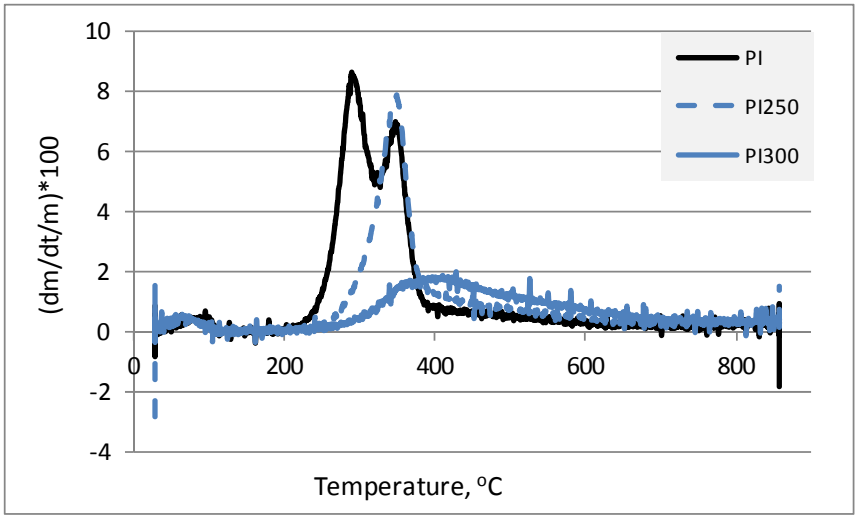

Figure 2. DTG curves of weight loss rate versus temperature for pistachio shells PI and biochars PI250 and PI300

XRD analysis

Figure 3 shows the XRD patterns of pistachio shell (PI) as well as of selected biochars PI300 and PI550. Cellulose, which is one of the important structural components of the primary cell wall of green plants, is detected in PI and is also present in biochars PI300 and PI550. Thermonatrite, the naturally occurring evaporite mineral form of sodium carbonate, is present in PI as a result of atmospheric carbonation, while this phase is not present in biochars PI300 and PI550 due to the higher pyrolysis temperature.

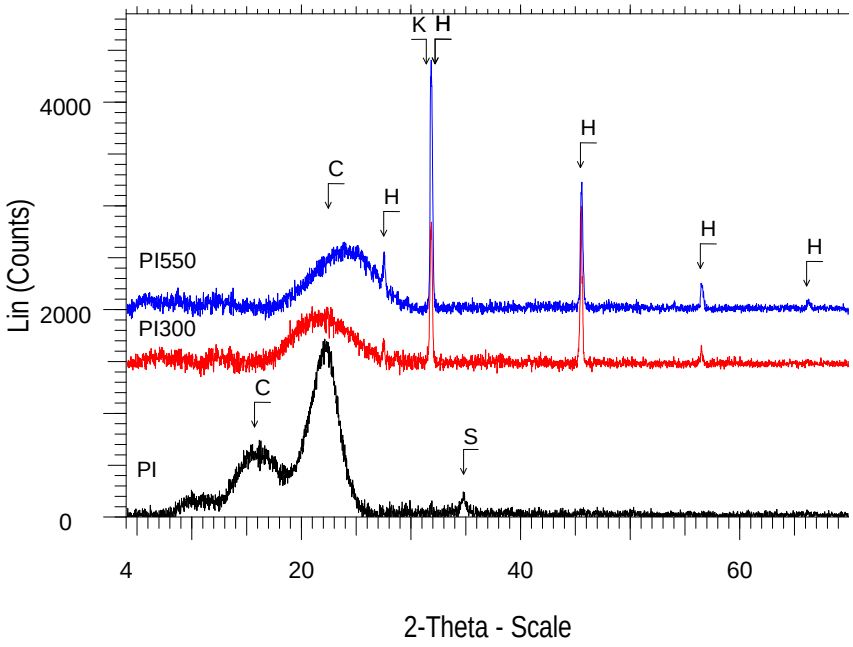

Figure 3. XRD patterns of pistachio shells PI and biochars PI300, PI550 (C: cellulose $(C_6H_{10}O_5)_n$, H: halite (NaCl), K: kalicinite ($KHCO_3$), S: thermonatrite ($Na_2CO_3H_2O$))

The XRD patterns of PI300 and PI550 are quite similar and are characterized by the elevated background between 16 to 26° 2-theta, due to the presence of organic matter [32]. Halite is present in biochars PI300 and PI550, as a residual phase which can be more easily detected by XRD as a result of decomposition of organic phases in temperatures higher than 300 °C. The presence of halite is due to residual salt that was not fully removed during soaking of the raw material. The presence of kalicinite, detected in PI300 and PI550, improves the quality of biochar. Kalicinite, which is mainly formed in nature after decomposition of dead trees, is a highly soluble mineral phase and may be involved in a) release of K in soil when biochar is added as amendment and b) exchange of K with divalent ions if biochar is used as adsorbent.

FTIR analysis

Figure 4 shows the FTIR spectra of pistachio shells PI and biochars PI300, PI550. FTIR spectra band assignments are presented in Table 2.

The broad peaks seen for all samples at around 3430 cm^{-1} indicate the presence of hydroxyl group (−OH) stretching. The peaks at 2850 and 2920 cm^{-1}, also seen in all samples, are ascribed to aliphatic C−H deforming vibration [33, 34].

The band at 1735 cm^{-1} for PI, which is slightly shifted for PI300 and PI550 to 1700 cm^{-1}, is assigned to ν(C=O) vibration in carbonyl group or the presence of carboxylic bonds [32, 35]. The intensity of these bands decreases at higher temperatures due to the decomposition of carbonate compounds. The bands at around 1600 cm^{-1} are due to the presence of aromatic C=O ring stretching (likely –COOH) or C=C stretching of aromatic groups in lignin implying the presence of residual lignin after decomposition. These bands are stronger in the spectra derived at higher temperatures, as expected from the respective pH values, provide alkalinity and increase pH if biochar is used as amendment in acidic soils. It is mentioned that the exact position of the peaks around 1600-1700 cm^{-1} is related to the conjunction of the carbonyl groups with the aromatic ring. The ratio of these peaks has been also found to reflect the degree of charring of cellulose [36, 37].

The characteristic peaks of the aromatic C=O ring stretching appear at 1500-1430 cm^{-1}. The band at 1385 cm^{-1} is attributed to δ(C=H) vibration in alkanes and alkyl groups [38]. The band at 1260 cm^{-1}, which is mainly seen in PI and

almost disappears in PI300 and PI550, is attributed to C=C stretching. These bands decrease with increasing temperature, as also shown by CaO and Harris [32].

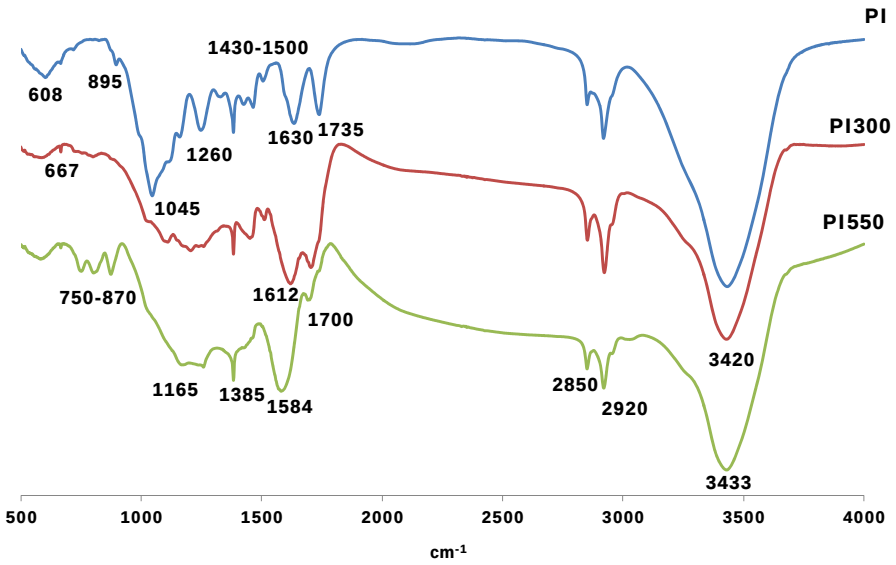

Figure 4. FTIR spectra of pistachio shell PI and biochars PI300, PI550

Table 2. FTIR spectra band assignments

Band number, cm^{-1}	Assignment
3433, 3420	Hydroxyl group (−OH) stretching
2850, 2920	Aliphatic C−H deforming vibration
1735, 1700	ν(C=O) vibration in carbonyl group or presence of carboxylic bonds
1630, 1612, 1584	Aromatic C=O ring stretching (likely –COOH) or C=C stretching of aromatic groups in lignin
1500-1430	Aromatic C=O ring stretching
1385	δ(C=H) vibration in alkanes and alkyl groups
1260	C=C stretching
1045, 1165	Aliphatic ether, alcohol C−O or aromatic stretching peak, O−H deformation vibrations, b-glycosidic bond in cellulose and hemicellulose
800-600	C–H wagging vibrations

The sharp peak shown at 1045 cm^{-1} in PI and the smaller peaks at around 1165 cm^{-1} in biochars PI300 and PI550 are due to aliphatic ether, alcohol C−O or aromatic stretching, O−H deformation vibrations or b-glycosidic bonds in cellulose and hemicelluloses. These functional groups disappear at temperatures higher than 300 ^{o}C indicating the decomposition of hemicellulose and cellulose [39, 40].

In the region 800-600 cm^{-1} aromatic and heteroaromatic compounds are confirmed by C–H wagging vibrations. The intensity of these peaks increases for PI550 due to the stability of these compounds and possible cyclisation. It is also mentioned that the stability of biochar is depended upon the transformation of the native carbon structure to polycyclic aromatic structures during pyrolysis resulting in high resistance against physical and microbial breakdown when biochar is applied on soils [41].

SEM analysis

In Figure 5, SEM backscattered electron images (BSI) of PI and biochars PI300 and PI550 are shown. It is seen from Figure 5a that the matrix of pistachio shell PI is heterogeneous containing particles with varying size (27.5-228 μm). When PI is pyrolized for the production of biochar at 300 ^{o}C (PI300) some agglomeration takes place and the particle size varies between 51.9 and 565 μm (Figure 5b).

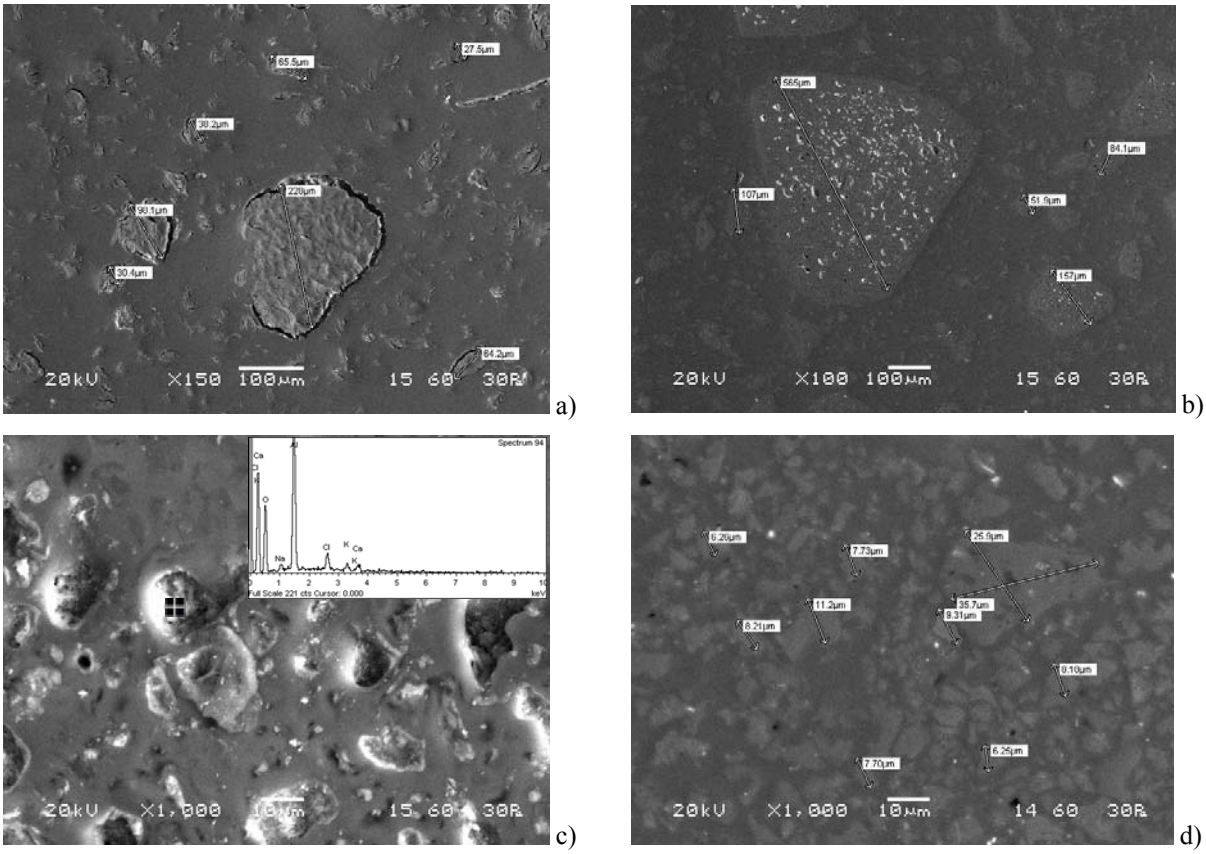

Figure 5. SEM-BSI images of a) PI (x150), b) PI300 (x100), c) representative EDS analysis of the PI300 pore structure and d) PI550 (x1000)

The examination of the porous structure of the biochars reveals a distribution of macropores with varying size and shape. These macropores with a bigger size in biochars compared to PI enclose a network of irregularly scattered micropores in the surface due to the release of volatiles. The EDS analysis (Figure 5c) of the surface of micropores identified high levels of Ca, Na, Cl, Al and K thus confirming the XRD patterns indicating that some associated mineral crystals, such as halite (NaCl) and kalicinite ($KHCO_3$), are present in biochars after pyrolysis at 300 ^oC. The presence of Al can be attributed to the use of ultra-fine corundum (Al_2O_3) powder for polishing of the samples prepared for SEM analysis.

It is also known that pyrolysis may be affected by the composition of the feedstock (content of holocellulose, lignin and inorganic matter) as well as by its particle size to a lesser degree. When the feedstock is very fine, agglomeration may take place in higher temperatures and this may in turn affect the porosity of the final product. This is why the grain size of the feedstock in the present study was not reduced aiming to maintain a sufficient rate of diffusion of volatiles through the char.

If the pyrolysis temperature is further increased to 550 ^oC (PI550), a more homogenous matrix is obtained and the grain size becomes smaller and varies between 6.25 and 35.7 μm (Figure 5d). This can be attributed to the decomposition of more volatile fractions that were not fully decomposed in temperatures below 500 ^oC.

Adsorption potential of biochar

Table 3 presents the % Pb and Cu adsorption in solutions for pistachio shell PI and biochars PI300 and PI550 when various Pb and Cu (15, 45, 70 and 150 $mg \cdot L^{-1}$) or adsorbent (1, 2, 5 and 10 $g \cdot L^{-1}$) concentrations are used. From the experimental data it is shown that Pb is adsorbed more efficiently compared to Cu on PI and both biochars PI550 and PI300. The highest % adsorption of Cu and Pb, almost 100% for both ions, is shown for 10 $g \cdot L^{-1}$ biochar PI550, when the initial Pb and Cu concentration in solution was 15 $mg \cdot L^{-1}$. Lower adsorbent concentrations result in reduced adsorption efficiencies. In addition, the % adsorption of heavy metals decreases with increasing heavy metal concentration to 77.2 and 62.8% for Pb and Cu respectively, when their initial concentration in solution was 150 $mg \cdot L^{-1}$. Lower adsorption efficiency for all heavy metal concentrations is shown for PI and PI300.

Table 3. % Pb and Cu adsorption for pistachio shell PI and biochars PI300 and PI550 for various Pb and Cu (15, 45, 70 and 150 mg·L^{-1}) or adsorbent (1, 2, 5 and 10 g·L^{-1}) concentrations (AC: activated carbon)

Adsorbent[1]	Pb and Cu concentration (mg·L^{-1})	% Pb adsorption	% Cu adsorption	*Adsorbent*	Adsorbent concentration (g·L^{-1})	% Pb adsorption[2]	% Cu adsorption[2]
PI	15	86.2	62.4	*PI*	1	31.4	30.9
	45	75.7	42.9		2	34.7	32.7
	70	44.3	41.8		5	40.0	38.2
	150	38.3	36.7		10	44.3	41.8
PI300	15	96.9	71.2	*PI300*	1	40.0	34.5
	45	73.9	57.1		2	45.7	42.7
	70	57.1	52.7		5	52.9	47.3
	150	49.7	37.8		10	57.1	52.7
PI550	15	99.7	99.6	*PI550*	1	42.9	40.9
	45	99.1	97.6		2	53.6	50.0
	70	85.7	83.6		5	67.1	63.6
	150	77.2	62.8		10	85.7	83.6
				AC	10	57.1	41.6

[1]Adsorbent concentration 10 g·L^{-1}, [2]initial heavy metal concentration: 70 mg·L^{-1} Pb and 70 mg·L^{-1} Cu

Activated carbon, which was used as control adsorbent with a concentration of 10 g·L^{-1}, shows quite similar adsorption efficiency for both metal ions with biochar PI300. It is worth mentioning though that PI550 shows much better adsorption efficiency for both Pb and Cu ions compared to activated carbon.

Figures 6 and 7 show the adsorption rates for Pb and Cu, in mg·g^{-1}·h^{-1}, for pistachio shell (PI) and biochars PI300 and PI550. It is seen from these figures that:

- For all adsorbents used the adsorption rate of Pb and Cu increases with increasing heavy metal concentration (Figure 6) and decreasing adsorbent concentration (Figure 7).
- The highest adsorption rate for both metal ion concentrations until equilibrium, namely 1.22 and 1.17 mg·g^{-1}·h^{-1} for Pb and Cu, respectively, is shown for PI550 at 1 mg·L^{-1} biochar concentration.
- The adsorption rate of Pb is higher than Cu for all adsorbent and initial heavy metal concentrations used.
- Activated carbon shows almost identical with biochar PI300 adsorption rates, 0.17 and 0.13 mg·g^{-1}·h^{-1}, for Pb and Cu respectively, when the initial heavy metal concentration is 70 mg·L^{-1}.

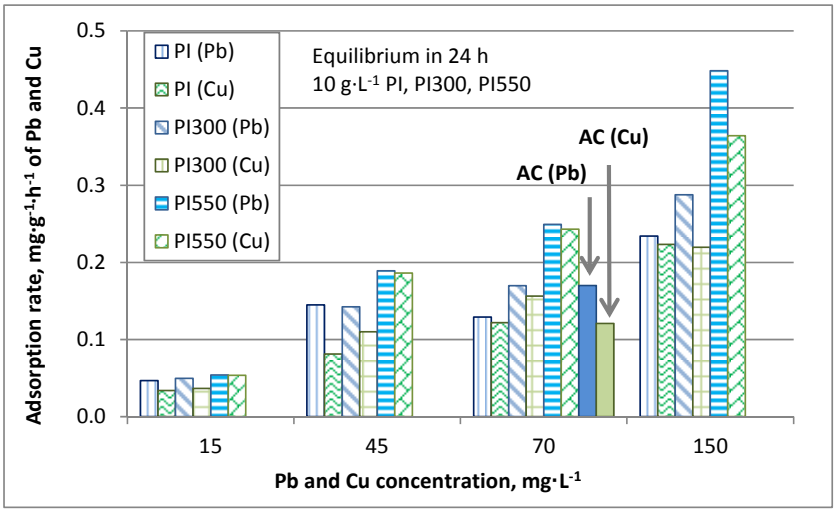

Figure 6. Adsorption rates, mg·g^{-1}·h^{-1}, of Pb and Cu (concentrations 15, 45, 70 and 150 mg·L^{-1}) for adsorbent (pistachio shell PI and biochars PI300, PI550) concentration 10 g·L^{-1} (AC: activated carbon, used as control)

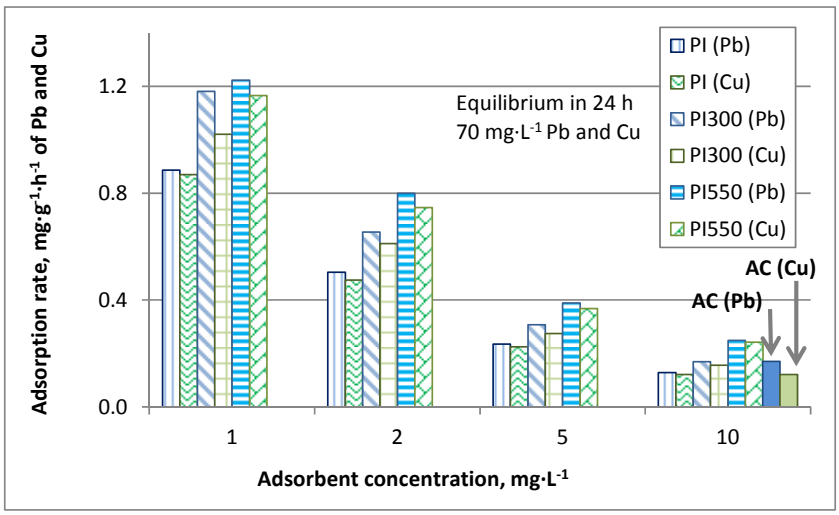

Figure 7. Adsorption rates, mg·g^{-1}·h^{-1}, of Pb and Cu (concentration 70 mg·L^{-1}) for adsorbent (pistachio shell PI and biochars PI300, PI550) concentrations 1, 2, 5 and 10 g·L^{-1} (AC: activated carbon, used as control)

The adsorption rate for PI and biochars PI300 and PI550 is quite well related to the ionic radius of each heavy metal ion studied (1.19 Å for Pb^{2+} and 0.73 Å for Cu^{2+}). Thus, the higher % adsorption is seen for Pb which has larger ionic radius than Cu. A similar trend is also noticed between adsorption rate and hydration enthalpy for each metal ion. The enthalpy of hydration of an ion, H_{hyd}, in kJ/mole, is the amount of energy released when a mole of the ion dissolves in a large volume of water forming thus an infinite dilute solution. It is shown that the higher the ionic radius the higher is the hydration enthalpy. The hydration enthalpy of Pb^{2+} is -1485 kJ/mole, considerably higher than that of Cu^{2+} (-2100 kJ/mole). These remarks have also been confirmed in previous studies [42, 43].

Therefore, it is deduced from the experimental data that the adsorption capacity of pistachio biochars increases with increasing pyrolysis temperature, as also reported by other researchers [44, 45]. The higher porosity and carbon content of biochar PI550 compared to PI300 is believed to contribute to its higher adsorption capacity. Similar behaviour has been reported for biochars produced from wetland plant residues [16, 23].

The Freundlich and Langmuir models have been used to describe adsorption. The Freundlich model is described by equation [1]

$$\log q_e = \log K_f + (1/n)\log C_e \quad [1]$$

where q_e (mg·g^{-1}) is the uptake of metal per unit weight of adsorbent in equilibrium, C_e (mg·L^{-1}) is the equilibrium concentration of metal ion in solution, K_f (L·g^{-1}) is the constant related to the adsorption capacity of the adsorbent and 1/n is the constant related to the adsorption intensity.

The Langmuir model is described by equation [2]

$$C_e/q_e = (1/bq_{max}) + (1/q_{max})C_e \quad [2]$$

where C_e (mg·L^{-1}) is the equilibrium concentration of metal ion in solution, q_e (mg·g^{-1}) is the uptake of metal per unit weight of adsorbent in equilibrium, q_{max} is the maximum adsorption capacity of the adsorbent (mg·g^{-1}) and b (L·mg^{-1}) is the Langmuir constant related to the energy of the adsorption.

The Freundlich and Langmuir isotherm constants, as well as the correlation coefficients R^2, were calculated based on the experimental data regarding adsorption of Pb and Cu using PI and biochars PI300 and PI550 in a solution containing 70 mg·L^{-1} Pb and 70 mg·L^{-1} Cu (Table 4).

Table 4. Freundlich and isotherm Langmuir constants for Pb and Cu removal of pistachio shell PI and biochars PI300 and PI550

	Pb						Cu					
	Freundlich			Langmuir			Freundlich			Langmuir		
	$\log K_F$	1/n	R^2	b	q_{max}	R^2	$\log K_F$	1/n	R^2	b	q_{max}	R^2
PI	-14.336	9.307	0.994	-0.020	-0.877	0.970	-17.147	10.930	0.973	-0.020	-0.690	0.967
PI300	-7.8663	5.741	0.998	-0.023	-2.082	0.911	-8.521	5.988	0.968	-0.021	-1.802	0.869
PI550	-0.3847	1.103	0.883	-0.006	-73.529	0.140	-0.508	1.146	0.857	-0.007	-55.866	0.156

According to the values shown in Table 4, experimental data fit very well the Freundlich model which proposes a monolayer sorption with heterogeneous energetic distribution of active sites, accompanied by interactions between adsorbed ions.

Conclusions

The present study shows that pistachio shells can be pyrolysed for the production of biochar that can be used both as soil amendment and adsorbent for the clean-up of solutions containing heavy metals such as Pb and Cu. Pyrolysis temperature was found to significantly affect biochar properties. Increased temperature results in increased char and fixed carbon content and decreased pyrolysis yield and volatile matter content. Increased temperature results also in increased pH values for the biochars produced and thus over the temperature range 220-650 ^{o}C pH increases from 3.3 to 8.8, indicating that different biochar qualities may be applied as amendment to different soil types, either alkaline or acidic.

The use of analytical techniques, namely TG, XRD, FTIR and SEM, offers significant insights regarding the composition and the morphology of the produced biochars. DTG confirms the pyrolysis of lignocellulose materials. XRD patterns indicate the presence of cellulose, kalicinite and residual halite. FTIR confirms the presence of functional groups such as carboxylic bonds and aromatic C=O ring stretching (likely –COOH) that provide alkalinity at higher pyrolysis temperatures. SEM analysis provides useful information on the homogeneity of the matrix and the porous structure of the produced biochars and shows that agglomeration takes place when pistachio cells are pyrolysed at higher temperature, mainly after 300 ^{o}C. More specifically, the examination of the porous structure reveals a distribution of macropores with varying size and shape. These macropores have a bigger size at increased pyrolysis temperature and enclose a network of irregularly scattered micropores in the surface due to the release of volatiles.

Pyrolysis temperature affects positively the biochar capacity in terms of Pb and Cu adsorption and subsequent removal from solutions. Biochars produced at 550 ^{o}C show high Pb and Cu adsorption capacity, which is much better than that of commercial activated carbon and is related to biochar properties such as high carbon content and porosity. The highest adsorption rate for both metal ion concentrations, namely 1.22 and 1.17 $mg \cdot g^{-1} \cdot h^{-1}$ for Pb and Cu, respectively, is shown for PI550 at 1 $mg \cdot L^{-1}$ biochar concentration. The experimental data fit very well the Freundlich model.

Acknowledgements

This research has been co-funded by the European Union (European Social Fund) and Greek National Resources through the Operational Program "Education and Lifelong Learning" of the National Strategic Reference Framework (NSRF) – Research Funding Program: THALES, Sub-project "Development of an integrated methodology for the management, treatment and valorisation of hazardous waste (WasteVal)" (code MIS 380038). Investing in knowledge society through the European Social Fund.

References

1. Kookana, R.S., Sarmah, A.K., Van Zwieten, L., Krull, E., Singh, B.: Biochar application to soil: agronomic and environmental benefits and unintended consequences. Adv. Agron. 112, 103–143 (2011)
2. Edmunds, C.W.: The Effects of Biochar Amendment to Soil on Bioenergy Crop Yield and Biomass Composition. MSc thesis, University of Tennessee, USA, http://trace.tennessee.edu/utk_gradthes/1150/ (2012). Accessed 24 April 2014
3. Manyà, J.: Pyrolysis for Biochar Purposes: A Review to Establish Current Knowledge Gaps and Research Needs. Environ. Sci. Technol. 46, 7939−7954 (2012)
4. Laird, D.A., Brown, R.C., Amonette, J.E., Lehmann, J.: Review of the pyrolysis platform for coproducing bio-oil and biochar. Biofuels Bioprod. Bior. 3, 547−562 (2009)
5. Novak, J.M., Lima, I., Xing, B., Gaskin, J.W., Steiner, C., Das, K.C., Ahmedna, M., Rehrah, D., Watts, D.W., Busscher, W.J., Schomberg H.: Characterization of designer biochar produced at different temperatures and their effects on a loamy sand. Ann. Environ. Sci. 3, 195–206 (2009)
6. Sánchez, M.E., Lindao, E., Margaleff, D., Martínez, O., Morán A.: Pyrolysis of agricultural residues from rape and sunflowers: Production and characterization of bio-fuels and biochar soil management. J. Anal. Appl. Pyrolysis 85, 142–144 (2009)
7. Kinney, T.J., Masiello, C.A., Dugan, B., Hockaday, W.C., Dean, M.R., Zygourakis, K., Barnes R.T.: Hydrologic properties of biochars produced at different temperatures, Biomass Bioenerg. 41, 34−43 (2012)

8. Dias, B.O., Silva, C.A., Higashikawa, F.S., Roig, A., Sanchez-Monedero, M.A.: Use of biochar as bulking agent for the composting of poultry manure: Effect on organic matter degradation and humification. Bioresource Technol. 101, 139–1246 (2010)

9. Stavi, I.: The potential use of biochar in reclaiming degraded rangelands. J. Environ. Plann. Man. 55, 657–665 (2012)

10. Bourne, D., Fatima, T., van Meurs, P., Muntean, A.: Is adding charcoal to soil a good method for CO_2 sequestration? - Modeling a spatially homogeneous soil. Appl. Math. Model. 38(9-10), 2463–2475 (2014)

11. Downie, A., Lau, D., Cowie, A., Munroe, P.: Approaches to greenhouse gas accounting methods for biomass carbon. Biomass Bioenerg. 60, 18–31 (2014)

12. Cabrera, A., Cox, L., Spokas, K., Hermosín, M.C., Cornejo, J., Koskinen, W.C.: Influence of biochar amendments on the sorption–desorption of aminocyclopyrachlor, bentazone and pyraclostrobin pesticides to an agricultural soil. Sci. Total Environ. 470–471, 438–443 (2014)

13. Jia, F., Gan, J.: Comparing black carbon types in sequestering polybrominated diphenyl ethers (PBDEs) in sediments. Environ. Pollut. 184, 131–137 (2014)

14. Inyang, M., Gao, B., Zimmerman, A., Zhang, M., Chen, H.: Synthesis, characterization, and dye sorption ability of carbon nanotube-biochar nanocomposites. Chem. Eng. J. 236, 39–46 (2014)

15. Agrafioti, E., Kalderis, D., Diamadopoulos, E.: Arsenic and chromium removal from water using biochars derived from rice husk, organic solid wastes and sewage sludge. J. Environ. Manage. 133, 319–314 (2014)

16. Ding, W., Dong, X., Ime, I.M., Gao, B., Ma, L.Q.: Pyrolytic temperatures impact lead sorption mechanisms by bagasse biochars. Chemosphere 105, 68–74 (2014)

17. Yang, G.-X., Jiang, H.: Amino modification of biochar for enhanced adsorption of copper ions from synthetic wastewater. Water Res. 48, 396–405 (2014)

18. Yetilmezsoy, K., Demirel, S.: Artificial neural network (ANN) approach for modeling of Pb(II) adsorption from aqueous solution by Antep pistachio (Pistacia Vera L.) shells. J. Hazard. Mater. 153, 1288–1300 (2008)

19. Moussavi, G., Khosravi, R.: Preparation and characterization of a biochar from pistachio hull biomass and its catalytic potential for ozonation of water recalcitrant contaminants. Bioresource Technol. 119, 66–71 (2012)

20. USEPA: Toxicity Characteristics Leaching Procedure (TCLP). Method 1311, Revision 0 (November 1990)

21. Antal Jr., M.J., Grønli, M.: The art, science, and technology of charcoal production. Ind. Eng. Chem. Res. 42, 1619–1640 (2003)

22. Amonette, J.E., Joseph. S.: Characteristics of biochar: Microchemical properties. In: Lehmann JL, Joseph S. eds. Chapter 3 in Biochar for Environmental Management: Science and Technology, London, Earthscan, 33–52 (2009)

23. Dai, Z., Meng, J., Muhammad, N., Liu, X., Wang, H., He, Y., Brookes, P.C., Xu, J.: The potential feasibility for soil improvement, based on the properties of biochars pyrolyzed from different feedstocks. J. Soils Sediments 13, 989–1000 (2013)

24. Deenik, J.L., McClellan, T., Uehara, G., Antal, M.J., Campbell, S.: Charcoal volatile matter content influences plant growth and soil nitrogen transformations. Soil Sci. Soc. Am. J. 74, 1259−1270 (2010)

25. Brewer, C.E., Chuang, V.J., Masiello, C.A., Gonnermann, H., Gao, X., Dugan, B., Driver, L.E., Panzacchi, P., Zygourakis, K., Davies, C.A.: New approaches to measuring biochar density and porosity. Biomass Bioenerg. (2014) doi: 10.1016/j.biombioe.2014.03.059

26. Gray, M., Johnson, M.G., Dragila, M.I., Kleber, M.: Water uptake in biochars: The roles of porosity and hydrophobicity. Biomass Bioenerg. 61, 196−205 (2014)

27. Gaskin, J.W., Steiner, C., Harris, K., Das, K.C., Bibens, B.: Effect of low-temperature pyrolysis conditions on biochar for agricultural use. Transactions of the ASABE 51, 2061–2069 (2008)

28. Steinbeiss, S., Gleixner, G., Antonietti, M.: Effect of biochar amendment on soil carbon balance and soil microbial activity. Soil Biol. Biochem. 41(6), 1301−1310 (2009)

29. Fisher, T., Hajaligol, M., Waymack, B., Kellogg, D.: Pyrolysis behaviour and kinetics of biomass derived materials. J. Anal. Appl. Pyrolysis 62, 331–349 (2002)

30. Ververis, C., Georghiou, K., Christodoulakis, N., Santas, P., Santas, R.: Fiber dimensions, lignin and cellulose content of various plant materials and their suitability for paper production. Ind. Crops Prod. 19, 245–254 (2004)

31. Vamvuka, D., Sfakiotakis S.: Effects of heating rate and water leaching of perennial energy crops on pyrolysis characteristics and kinetics. Renew. Energ. 36, 2433–2439 (2011)

32. Cao, X., Harris, W.: Properties of dairy-manure-derived biochar pertinent to its potential use in remediation. Bioresource Technol. 101, 5222–5228 (2010)

33. Yaman, S.: Pyrolysis of biomass to produce fuels and chemical feedstocks. Energ. Convers. Manage. 45, 651–671 (2004)

34. Liu Z., Quek, A., Hoekman, S.K., Balasubramanian, R.: Production of solid biochar fuel from waste biomass by hydrothermal carbonization. Fuel 103, 943–949 (2013)

35. Sharma, R.K., Wooten, J.B., Baliga, V.L., Lin, X., Geoffrey Chan, W., Hajaligol, M.R.: Characterization of chars from pyrolysis of lignin. Fuel 83, 1469−1482 (2004)

36. Pastorova, I., Botto, R.E., Arisz, P.W., Boon, J.J.: Cellulose char structure e a combined analytical Py-GC-MS, FTIR, and NMR study. Carbohydr. Res. 262, 27−47 (1994)

37. Chen, B., Chen, Z., Lv, S.: A novel magnetic biochar efficiently sorbs organic pollutants and phosphate. Bioresource Technol. 102, 716–723(2011)

38. Caglar, A., Demirbas, A.: Conversion of cotton cocoon shell to liquid products by pyrolysis. Energ. Convers. Manage. 41, 1749−1756 (2000)

39. Hossain, M.K., Strezov, V., Chan, K.Y., Ziolkowski, A., Nelson, P.F.: Influence of pyrolysis temperature on production and nutrient properties of wastewater sludge biochar. J. Environ. Manage. 92, 223–228 (2011)

40. Angin, D., Köse, T.E., Selengil, U.: Production and characterization of activated carbon prepared from safflower seed cake biochar and its ability to absorb reactive dyestuff. Appl. Surf. Sci. 280, 705–710 (2013)

41. Glaser, B., Haumaier, L., Guggenberger, G., Zech, W.: The 'Terra Preta' phenomenon: a model for sustainable agriculture in the humid tropics. Naturwissenschaften 88, 37−41 (2001)

42. Panayotova, M., Velikov, B.: Kinetics of heavy metal ions removal by use of natural zeolite. J. Environ. Sci. Heal. A 37(2), 139−147 (2002)

43. Caputo, D., Pepe, F.: Experiments and data processing of ion exchange equilibria involving Italian natural zeolites: a review. Micropor. Mesopor. Mat. 105, 222–231 (2007)

44. Chun, Y., Sheng, G.Y., Chiou, C.T., Xing, B.: Compositions and sorptive properties of crop residue-derived chars. Environ. Sci. Technol. 38, 4649−4655 (2004)

45. Wang, X., Sato, T., Xing, B.: Competitive sorption of pyrene on wood chars. Environ. Sci. Technol. 40, 3267−3272 (2006)